Research Article

Journal of Environmental Nanotechnology

Optimization of Anodization Time for TiO_2 Nanotubes and their Antibiofilm Activity against *Staphylococcus aureus* and *Pseudomonas aeruginosa*

R. Hemalin Subala[1,9], D. Henry Raja[1,9], N. SheenKumar[2], D. Jonas Davidson[3], M. Amalanathan[4*,9], M. Sony Michael Mary[5,9], V. S. Shali[5,9], D. Shiney Manoj[6], A. Seema[7] and lexmi S.[8]

[1]Department of Physics, Scott Christian College, Nagercoil, TN, India
[2]Department of Physics, St Xavier's Catholic College of Engineering, Nagercoil, TN, India
[3]CSIR-CECRI, Karaikudi, TN, India
[4]Department of Physics and Research Centre, Nanjil Catholic College of Arts and Science, Kaliyakkavilai, TN, India
[5]Department of Physics, Annai Velankanni College, Tholayavattam, TN, India
[6]Department of Physics, Christian College, Kattakada, Thiruvananthapuram, KL, India
[7]Department of chemistry, Mar Ephraem College of Engineering and Technology, Elavuvilai, Kanyakumari, TN, India
[8]Departmentof Physics, Sanatana Dharma College Alappuzha, KL, India
[9]Affiliated to Manonmaniam Sundaranar University, Abishekapatti, Tirunelveli, TN, India
Received: 26.09.2025 Accepted: 12.11.2025 Published: 30.03.2026
*nathan.amalphysics@gmail.com

ABSTRACT

This study presents a novel investigation into the synthesis and optimization of titanium dioxide nanotube (TiO_2) nanotubes (TNTs) fabricated via electrochemical anodization at varying times (1, 2, and 3 hours) under a constant 20V potential. Comprehensive characterization by FESEM, XRD, and EDX confirmed the formation of highly ordered anatase-phase nanotubes, with the 2-hour anodization condition yielding the most uniform morphology and superior antibacterial efficiency. Anti-biofilm activity was assessed against *Staphylococcus aureus* and *Pseudomonas aeruginosa* using Microtitre Plate Assay, showing significant inhibition rates of 45.7% and 61.18% at 500 ug/mL, respectively, compared to controls. These findings underscore the optimized time's critical role in enhancing TiO_2 nanotubes antibiofilm properties. Furthermore, the study highlights potential improvements through incorporating silver and graphene nanocomposites to further boost antimicrobial performance, marking a significant advancement in biomedical implant surface modification.

Keywords: Titanium dioxide; Nanotubes; Anodization; Biofilm inhibition; Antimicrobial nanomaterials; *Staphylococcus aureus; Pseudomonas aeruginosa*.

1. INTRODUCTION

Microbial infections remain a critical global health issue, especially due to the formation of persistent biofilms on medical devices and human tissues. Pathogens such as *Staphylococcus aureus* and *Pseudomonas aeruginosa* are known for their ability to form resilient biofilms that protect them from host immune responses and antibiotic treatments, leading to chronic infections and healthcare-associated complications. Biofilm-related infections pose a significant global health risk, particularly with the rising use of invasive medical devices, leading to post-operative complications and device malfunctions (Pollán *et al.* 2020). Nanotechnology offers promising solutions in this regard, with titanium dioxide (TiO_2) nanostructures attracting significant attention for their antimicrobial activity (Opolot *et al.* 2024; Kunrath *et al.* 2024; Jedi-soltanabadi *et al.* 2018). TiO_2 exists in anatase, rutile, and brookite phases, with anatase being the most effective photocatalyst (Aravind *et al.* 2021a). Upon light activation, TiO_2 produces reactive oxygen species that damage bacterial cells, leading to broad-spectrum and sustained antimicrobial effects (Jedi-soltanabadi *et al.* 2018). These properties have led to its application in antibacterial coatings, self-cleaning surfaces, and biomedical devices.

The goal of this research is to create nanotubes with specific properties by optimizing anodization parameters, including time, voltage, annealing temperature, and electrolyte composition. By creating well-aligned nanotubes through field-assisted oxidation, migration, and dissolution processes, anodization

improves a material's performance by forming an oxide layer on its surface. TiO_2 nanotubes have a number of benefits over other nanostructures, such as spheres, sheets, rods, and wires, thanks to their shape, which resembles test tubes with an open top and a closed, curved bottom. A high surface-to-volume ratio and reduced charge carrier recombination rates (electron-hole pairs) are two of these benefits (Rathi *et al.* 2018; Pollan *et al.* 2020; Surya *et al.* 2020; Farrell *et al.* 2007). The anodization process is simple, cost-effective, and allows precise control over growth parameters, such as potential, pH, electrolyte chemistry, and time. These parameters strongly influence the chemical and physical properties of anodic TiO_2 nanotubes, enabling the modification of the nanotube morphology to achieve the desired characteristics (Raja and Arsha, 2024; Mohan *et al.* 2020). Research has shown that anodization time significantly affects nanotube morphology, with more extended anodization periods resulting in longer nanotubes (Montakhab *et al.* 2020; Kahlmeter, 2003). Furthermore, applying agitation during anodization can have detrimental effects on the surface ordering and synthesis of nanograss-free TNTs (Torres *et al.* 2023; Ayal, 2019; Chernozem *et al.* 2016; Garg *et al.* 2022; Han *et al.* 2009; Mazzarolo *et al.* 2012; Meyer *et al.* 2003).

The present study aims to optimize the anodization parameters, particularly anodization time, to synthesize TiO_2 nanotubes and evaluate their anti-biofilm activity. This research will contribute to developing TiO_2-based materials with enhanced antimicrobial properties for combating biofilm-related infections, particularly those caused by *S. aureus* and *P. aeruginosa*.

2 MATERIALS AND METHODS

2.1 Materials

The anode was made of analytical-grade, 99.7% pure titanium foil that measuring 3 cm by 1 cm (L x W) with a thickness 0.25 mm. It was procured from Sigma-Aldrich, United States. Analytical-grade ethylene glycol ($C_2H_6O_2$, 99%) and ammonium fluoride (NH_4F, 98%) were obtaining from SRL Chemicals to prepare electrolyte solutions. These chemicals were used as received without further purification. A DC power unit (Aplab) was employed to apply the potential, and deionized water from the Millipore Milli-Q system was used throughout all experiments.

2.2 Synthesis of Time-varying TiO_2Nanotubes

The titanium surface was mechanically polished and the foil was thoroughly cleaned with ethanol and distilled water to get rid of contaminants. Platinum was chosen as the cathode and dry titanium foil as the anode in an electrochemical cell. All reactions were carried out at room temperature (27°C). At least 2.5 centimeters separated the two electrodes. The DC power supply's positive and negative terminals were linked to the platinum and titanium electrodes, respectively. An organic electrolyte was made in order to create the TiO_2nanotubes. Ethylene glycol, 0.5 wt% % NH_4F, and 2 vol% H_2O make up the solution. To prevent unintended reactions, the titanium foil was insulated on all surfaces except a defined area 1 cm^2, which was left exposed to the electrolyte. Parafilm and Scotch tape were used as insulating materials. Three distinct anodization times—one, two, and three hours—were used in the experiment, all while keeping the anodization potential constant at 20V. After post-treatment, the samples were rinsed with ethanol and a tiny bit of distilled water to get rid of the sediments. For the produced NTs to successfully form a crystalline structure, they were annealed at 430°C. The samples were labelled as H_1, H_2, and H_3, corresponding to anodization times of one, two, and three hours, respectively.

2.3 Characterization Methods

The morphology and elemental content of the photoanodes were investigated using Field Emission Scanning Electron Microscopy (FESEM, Apreo S LoVac, Thermo Fisher scientific), which was powered by an EDX and operated at a voltage of about 20 KV. Using a D8 ADVANCE Bruker apparatus and Cu Kα radiation (λ=1.5417Å), X-ray diffraction (XRD) was used to investigate the crystal structure and phase purity of the produced photoanodes. X'Pert High Score software was then used for analysis.

2.3.1 Microtitre Plate Assay (MTP) for Biofilm Inhibiion

Sessile bacterial adhesion was quantified using the microtiter plate assay following the method described by (O'Toole, 2011). Briefly, 96-well flat-bottom polystyrene microtiter plates were filled with 180 µL of Brain Heart Infusion (BHI) broth, and 10 µL of an overnight culture of the pathogenic bacteria was added to each well. Test samples (sample H_3) were added at concentrations ranging from 500 to 0.9 µg/mL, in 10 µL volumes, alongside control wells without test samples. Following inoculation, the plates were incubated at 370C for 24 hours to allow biofilm formation. After incubation, the content of each well was carefully removed, and the wells were rinsed with 0.2 mL of phosphate-buffered saline (PBS, pH 7.2) to remove loosely attached bacteria

$$\% \text{ Biofilm inhibition } = \frac{\text{Control OD} - \text{Test OD}}{\text{Control OD}} \text{X } 100 \quad \ldots (1)$$

3. RESULTS AND DISCUSSION

The titanium foil exhibited a progressive color change from light grey to blue, then greenish-blue, and eventually purple during anodization. This color variation is caused by optical interference of light waves reflected from the varying thickness of the oxide layer (TiO_2) formed on the surface (Alipal *et al.* 2021). The

interference effects arise as the oxide layer thickness during anodization, resulting in constructive and destructive interference at different wavelengths that produce visible hues corresponding to the oxide thickness. This progressive color shift indicates the formation and growth of the anodic oxide layer, which correlates with the development of TiO_2 nanotubes.By employing diverse post-treatment techniques, Chin Lai *et al.* were able to produce TiO_2 nanotubes (TNTs) in a variety of morphologies. They displayed FESEM pictures of TNTs that had been cleansed by ultrasonography in water for a minute and then allowed to dry at room temperature. Remarkably, comparable pictures were also produced under ordinary circumstances by simply rinsing the nanotubes with pure water (Lai and Sreekantan, 2012).

3.1 FESEM Analysis

FESEM analysis confirmed the preparation of highly ordered TiO_2 nanotubes. This analysis examined the surface characteristics of the prepared samples.The chemical reaction involved in the anodization process can be described as follows (equation 2 and 3 below) (Brudzisz *et al.* 2021).

$$Ti^{4+} + 2H_2 \longrightarrow TiO_2 + 4e^- + 4H^+ \quad \ldots (2)$$

$$TiO_2 + 6\,NH_4F + 4\,H^+ \longrightarrow [TiF_6] + 2H_2O + 6NH_4^+ \quad \ldots (3)$$

At the onset of anodization, a dense oxide layer forms on the titanium surface as described by equation 2. Titanium metal is oxidized under an applied potential, allowing it to react with O_2^- ions from water (H_2O) to create the initial oxide layer. The subsequent thickening of this oxide layer is regulated by field-assisted ion transport, involving O_2^- from water in the electrolyte and Ti^{4+} ions from the underlying titanium. Since the oxide layer is highly resistive to charge flow, this reduces the electric field strength and results in a decrease in current. Concurrently, chemical etching of the oxide layer by fluoride ions (as shown in equation 3) leads to the development of a porous oxide layer, ultimately resulting in tubular structures through the continuous chemical dissolution of the field-assisted oxide layer. Fluoride ions can form a water-soluble TiF_6^{2-} complex, according to equation 3, which facilitates the dissolution of the formed TiO_2. Over time, this porous oxide layer deepens due to ongoing chemical etching, eventually leading to the formation of distinct tubular structures. By carefully adjusting the anodization parameters that influence both field-assisted oxidation and chemical etching reactions, we propose that the growth rate of the tubes can be optimized.

3.1.1 Effect of Anodization Time

The morphology and length of TiO_2 nanotubes (TNTs) play a crucial role in their antimicrobial performance. Controlling the geometrical parameters of the nanotubes, including their length and inner diameter, is essential. The tube length of TiO_2 NTs can be adjusted by varying the anodization time.

In this study, nanotube formation began at a voltage of 20V, aligning with previous research showing that nanotubes generally develop at voltages above 10V. A working voltage of 20V was chosen, and the nanotube diameter and wall thickness were regulated by varying the anodization time while maintaining a constant voltage and temperature. The nanotube dimensions—diameter, wall thickness, and length—were found to be highly influenced by the anodization time.

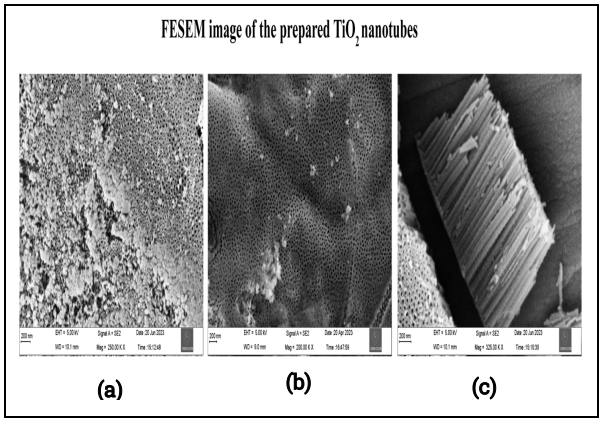


Fig. 1: Top view FESEM image of the samples prepared at (a)1 hour (b) 2 hours and (c)3 hours

As shown in Fig (1), the TiO_2 nanotube arrays exhibit a highly organized structure, with an average inner diameter of approximately 40 nm, as determined using ImageJ software. The most uniform porous structure was achieved at anodization times of 60 and 120 minutes. Continuous exposure to fluoride ions interacts within the pores, expanding them and facilitating the formation of aligned nanotubes. This reaction enhances the growth and overall organization of the nanotubes

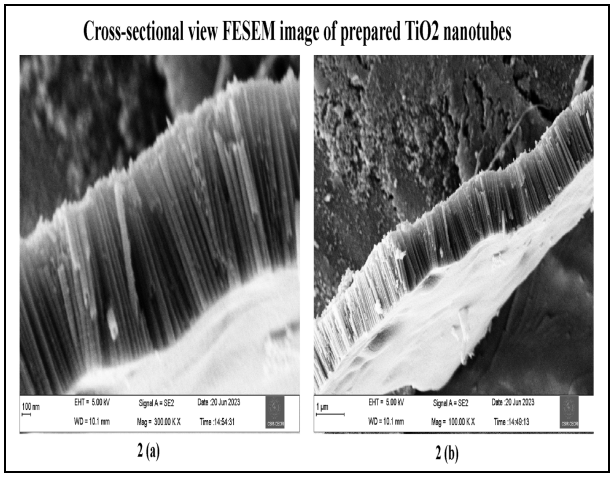


Fig. 2: Cross-sectional view FESEM image of the samples prepared at (a) 1 hour and (b) 2 hours

Table (1) presents the TNT tube length as a function of anodization time (Mahmud *et al.* 2015; Chernozem *et al.* 2016; Regonini *et al.* 2012; Bhadra et al. 2020; Aravind *et al.* 2021b). Increasing the anodization time to 180 minutes results in longer nanotubes, as shown in Figure (2). However, prolonged anodization leads to over-dissolution of the nanotube tops, causing structural degradation, as shown in Figure 3. While fluoride ion etching enlarges pores allowing nanotube elongation, overextended anodization causes pore wall thinning and top dissolution, accounting for the apparent contradiction pore expansion and nanotube narrowing. Initially, controlled anodization promotes the growth of uniform and well-defined nanotubes. However, excessive anodization can introduce detrimental effects. One primary issue is the increased heat generation during the process, which can disrupt nanotube stability. Elevated temperatures may induce thermal effects that distort the nanotubes, causing them to lose their original shape and develop irregularities.

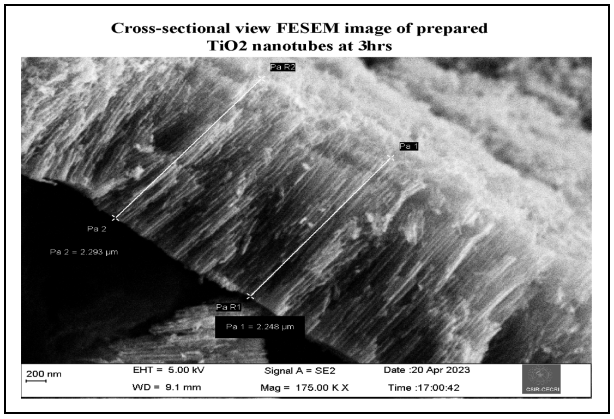


Fig. 3: Cross-sectional view FESEM image of the sample prepared at 3 hours

Table 1: Tube length vs anodization time at 20V

Sample	Anodization Time (minutes)	Anodization Voltage (V)	Tube Length (µm)
H_1	60	20	1.2
H_2	120	20	1.3
H_3	180	20	2.3

3.2 XRD Analysis

The anodized samples were analyzed for their phase composition and structure using X-ray diffraction (XRD). The identified diffraction peaks correspond to pure titanium metal (JCPDS No. 00-044-1294) and the TiO_2anatase phase (JCPDS No. 21-1272), closely resembling previously reported patterns for titanium and anatase TiO_2 are made in Fig.4.

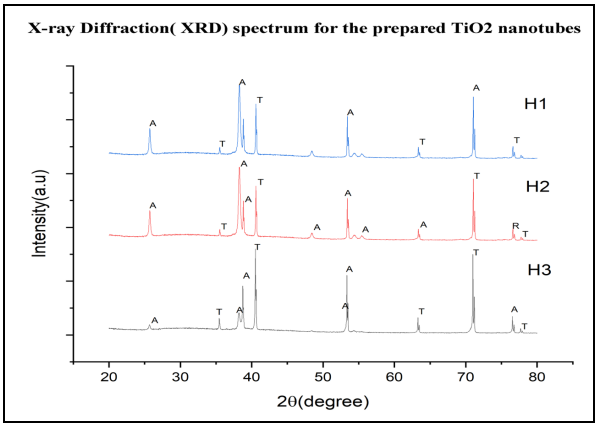


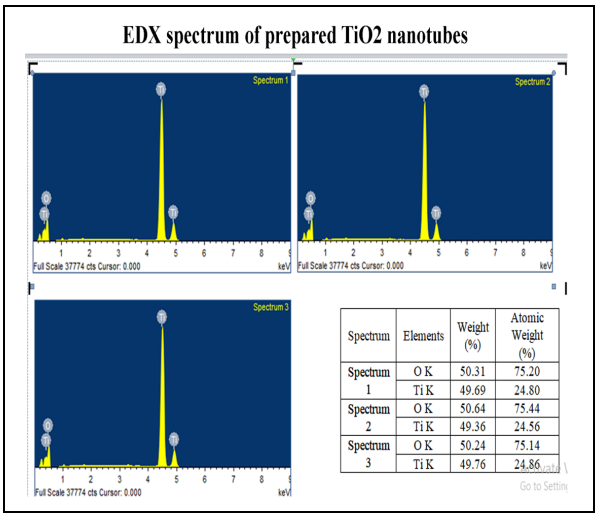
Fig. 4: X-ray diffraction (XRD) spectrum for the prepared samples

For sample H1, anodized for one hour, anatase phase peaks were observed at 2θ = 25.65°, 38.32°, 53.34°, and 71.18°, corresponding to the (101), (112), (105), and (220) planes, indicating a highly crystalline anatase TiO_2 phase. Titanium metal phase peaks were detected at 2θ = 38.32°, 40.53°, 63.35°, 70.95°, and 76.51°, corresponding to the (002), (101), (110), (103), and (112) planes.In sample H_2, anodized for two hours, anatase phase peaks appeared at 2θ = 38.62°, 38.78°, 53.18°, 53.3°, and 76.56°, indexed to the (112), (115), and (301)showing an increase in crystallinity with prolonged anodization time. The titanium metal phase was identified with peaks at 2θ = 35.4°, 40.53°, 63.30°, and 77.70°, corresponding to the (100), (101), (110), and (201) planes. For sample H_3, anodized for three hours, anatase phase peaks were found at 2θ = 25.70°, 38.25°, 38.83°, 48.39°, 53.41°, 55.41°, and 63.35°, indexed to the (101), (112), (200), (105), (211), and (204) planes, indicating a highly crystalline anatase phase. Titanium metal peaks appeared at 2θ = 35.5°, 40.5°, 71.0°, and 77.74°. Additionally, rutile phase peaks emerged at 2θ = 54.35° and 76.60° corresponding to the (211) and (301) planes, suggesting the onset of anatase-to-rutile phase transformation with extended anodization. This phase transformation is significant as anatse TiO_2 is often more photcatalytically active, whereas rutile has greater thermal stability, impacting the functional properties of the synthesized nanotubes. XRD analysis confirmed the crystalline nature of the resulting structure (Sun *et al.* 2016; Rojviroon *et al.* 2021; Abisharani *et al.* 2019, Chen *et al.* 2018, Abish *et al.* 2024).

Additionally, the XRD patterns verified that no other phases, like brookite, were present. The anodization process promoted the growth of the titanium oxide layer, resulting in a thin oxide layer relative to the substrate thickness. As a result, X-rays were able to penetrate the oxide layer easily, causing the titanium diffraction peaks to dominate.

3.3 Composition Analysis by EDX

An acceleration voltage of 15 keV was used in energy dispersive X-ray analysis to conduct elemental characterization of the resulting nanotubular layers. The EDX elemental analysis of the Titania NTs samples revealed only the presence of titanium and oxygen. As shown in the EDX spectra of the tube bundles in Fig.5, the composition consisted solely of titanium and oxygen. The use of organic electrolytes in the tube fabrication did not affect the composition of the samples. No signs of contamination were observed in the TNTs' EDX spectra. The presence of Ti and O atoms confirms the successful electro-anodization of titanium metal to TiO_2 (Amalanathan *et al.* 2022, Rahimpour *et al.* 2021).



Spectrum	Elements	Weight (%)	Atomic Weight (%)
Spectrum 1	O K	50.31	75.20
	Ti K	49.69	24.80
Spectrum 2	O K	50.64	75.44
	Ti K	49.36	24.56
Spectrum 3	O K	50.24	75.14
	Ti K	49.76	24.86

Fig. 5: EDX spectrum of the samples prepared at (a) 1 hour(b) 2 hours and (c) 3 hours

3.4 Antibiofilm Efficacy of TiO_2 Nanotubes Against *S. aureus and P. aeruginosa*

The antibiofilm efficacy of titanium dioxide (TiO_2) nanotubes was evaluated against *Staphylococcus aureus* (Gram-positive) and *Pseudomonas aeruginosa* (Gram-negative) by measuring optical density (OD) and calculating percentage inhibition at different concentrations. Statistical data are presented as mean OD values ± standard deviation (SD), with experiments performed in triplicate (n=3).

For *Staphylococcus aureus* at 500 µg/mL concentration, the mean OD was 1.868 ± 0.12, corresponding to a modest inhibition rate of 45.7%. This moderate inhibition aligns with the thick but porous peptidoglycan layer of Gram-positive bacteria, allowing partial interaction with TiO_2 nanotubes; however, robust antioxidative defense mechanisms potentially limit nanoparticle efficacy against biofilm formation. (Aravind *et al.* 2021).

In contrast, *Pseudomonas aeruginosa* showed a higher susceptibility. At 500 µg/mL, the mean OD was 0.771 ± 0.10, resulting in approximately 61.18% biofilm inhibition. Gram-negative bacteria possess this porous peptidoglycan layer and an outer membrane rich in lipopolysaccharides (LPS), which may facilitate enhanced interaction and nanoparticle entry, disrupting bacterial integrity. Moreover, oxidative stress from reactive oxygen species (ROS) generated by TiO_2 nanotubes contributes to this susceptibility.

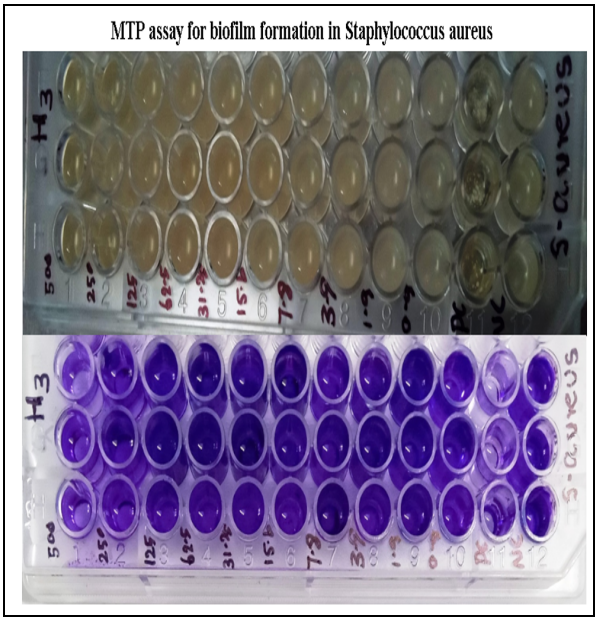


Fig. 6: MTP assay for biofilm formation in *Staphylococcus aureus* at different concentrations of TiO_2 nanotubes

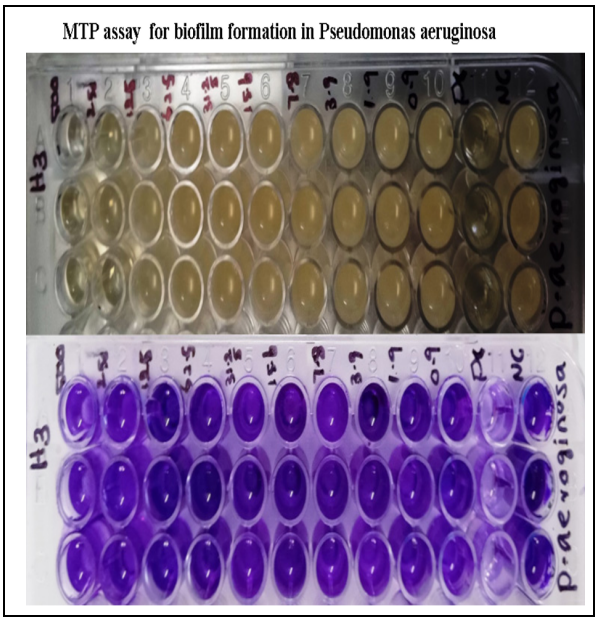


Fig. 7: MTP assay for biofilm formation in *Pseudomonas aeruginosa* at different concentrations of TiO_2 nanotubes

Table 2. presents the percentage inhibition of *Staphylococcus aureus* growth at different concentrations of TiO_2 nanotubes

S. No.	Tested Sample Concentration (µg/ml)	OD Value in 600 nm	Percentage of Inhibition (in Triplicates)			Mean Inhibition (%)
1.	Antibiotic	0.1043	95.424	95.702	96.502	95.876
2.	500 µg/ml	1.887	44.34	44.55	48.34	45.74
3.	250 µg/ml	2.222	0	0	0	0
4.	125 µg/ml	2.281	0	0	0	0
5.	62.5 µg/ml	2.710	0	0	0	0
6.	31.25 µg/ml	1.043	0	0	0	0

Figures 6-8 illustrate microtiter plate assays and optical density measurements, supporting these findings.

To enhance antibiofilm efficacy, future work will focus on TiO_2-based nanocomposites integrating silver and graphene. Silver nanoparticles are known for broad-spectrum antimicrobial action. And graphene disrupts biofilm structure significantly. Their combination with TiO_2 is expected to produce synergistic effects yielding superior antibiofilm performance, as supported by recent literature.

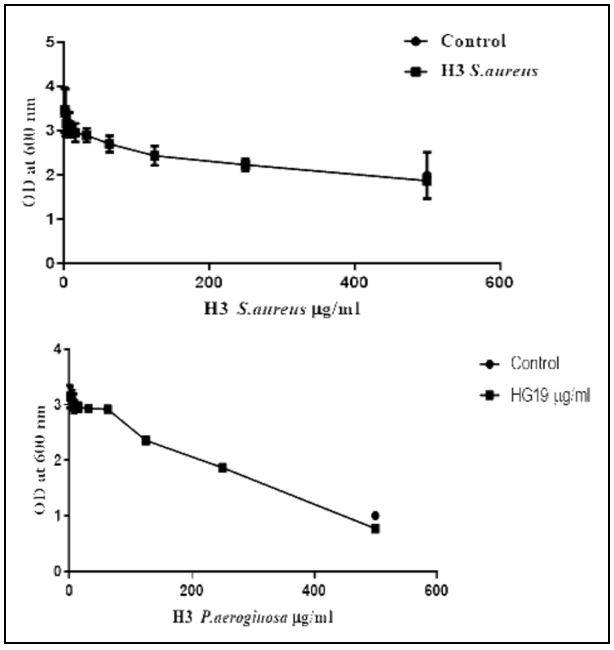


Fig. 8: OD measurements for biofilm formation in *Staphylococcus aureus* (top) and *Pseudomonas aeruginosa* (bottom) with TiO_2 nanotubes

4. CONCLUSION

This study successfully synthesized highly ordered TiO_2 nanotubes (TNTs) through anodization, with tunable morphology confirmed by FESEM and structural validation by XRD and EDX analyses showing pure anatase-phase TiO_2. The TiO_2 nanotubes exhibited concentration-dependent antibiofilm activity, demonstrating moderate inhibition of *Staphylococcus aureus* and limited notable effects against *Pseudomonas aeruginosa*. These differences reflect variations in bacterial cell wall composition and defense mechanisms. This work highlights the potential of TiO_2 nanotubes as versatile antibacterial materials and provides a foundation for further optimization through nanocomposite development.

FUNDING

This research received no specific grant from any funding agency in the public, commercial, or not-for-profit sectors.

CONFLICTS OF INTEREST

The authors declare that there is no conflict of interest.

COPYRIGHT

This article is an open-access article distributed under the terms and conditions of the Creative Commons Attribution (CC BY) license (http://creativecommons.org/licenses/by/4.0/).

REFERENCES

Abish, V. J., Raja, D. H. and Davidson, D. J., Na-deposited TiO_2 nanotubes for photo electrochemical water splitting with enhanced activity–A novel approach, *Mater. Lett.*, 362, 136210(2024). https://doi.org/10.1016/j.matlet.2024.136210

Abisharani, J. M., Devikala, S., Kumar, R. D., Arthanareeswari, M. and Kamaraj, P., Green synthesis of TiO_2 nanoparticles using Cucurbita pepo seeds extract, *Mater. Today: Proce.*, 14, 302-307(2019). https://doi.org/10.1016/j.matpr.2019.04.151

Alipal, J., Lee, T. C., Koshy, P., Abdullah, H. Z. and Idris, M. I., Evolution of anodised titanium for implant applications, *Heliyon,* 7(7), e07408 (2021). https://doi.org/10.1016/j.heliyon.2021.e07408

Amalanathan, M., Aravind, M., Ahmed, N., Mary, M. S. M., Velusamy, P., Kumaresubitha, T., Noreen, R. and Ali, S., The influence of activated carbon annealing temperature on sunlight-driven photocatalytic dye degradation and biological activity, *Inorg. Chem. Commun.,* 146, 110149 (2022). https://doi.org/10.1016/j.inoche.2022.110149

Aravind, M., Ahmad, A., Ahmad, I., Amalanathan, M., Naseem, K., Mary, S. M. M. and Zuber, M., Critical green routing synthesis of silver NPs using jasmine flower extract for biological activities and photocatalytical degradation of methylene blue, *J. Environ. Chem. Eng.,* 9(1), 104877(2021a). https://doi.org/10.1016/j.jece.2020.104877

Aravind, M., Amalanathan, M. and Mary, S. M. M., Synthesis of TiO_2 nanoparticles by chemical and green synthesis methods and their multifaceted properties, *SN Appl. Sci.,* 3, 409 (2021b). https://doi.org/10.1007/s42452-021-04281-5

Ayal, A. K., Effect of Anodization Duration in the TiO_2 Nanotubes Formation on Ti Foil and Photoelectrochemical Properties of TiO_2 Nanotubes, *J. Sci.,* 29(3), 77–81 (2019). https://doi.org/10.23851/mjs.v29i3.640

Bhadra, C. U., Davidson, D. J. and Raja, D. H., Fabrication of titanium oxide nanotubes by varying the anodization time, *Mater. Today: Proce.*, 33, 2711-2715(2020). https://doi.org/10.1016/j.matpr.2020.01.455

Brudzisz, A. M., Gizinski, D. and Stępniowski, W. J., Incorporation of Ions into Nanostructured Anodic Oxides—Mechanism and Functionalities, *Mol.*, 26(21), 16378 (2021). https://doi.org/10.3390/molecules26216378

Chen, S., Zhang, S., Tan, Z. and Zhang, S., Effect of Two-step Anodization on structure of TiO_2 Nanotube Arrays, *Adv. Func. Mater. Proce. China Mater. Conf.,* 18, 947-955(2017). https://doi.org/10.1007/978-981-13-0110-0_102

Chernozem, R. V., Surmeneva, M. A. and Surmenev, R. A., Influence of Anodization Time and Voltage on the Parameters of TiO_2 Nanotubes, *IOP Conf. Ser.: Mater. Sci. Eng.,* 116, 012025 (2016). https://doi.org/10.1088/1757-899X/116/1/012025

Farrell, D. J., File, T. M. and Jenkins, S. G., Prevalence and antibacterial susceptibility of mef (A)-positive macrolide-resistant Streptococcus pneumoniae over 4 years (2000 to 2004) of the PROTEKT US Study, *J. Clinic. Microbio.*, 45(2), 290-293(2007). https://doi.org/10.1128/JCM.01653-06

Garg, P., Attri, P., Sharma, R., Chauhan, M. and Chaudhary, G. R., Advances and Perspective on Antimicrobial Nanomaterials for Biomedical Applications, *Front. Nanotech*., 4, 898411 (2022). https://doi.org/10.3389/fnano.2022.898411

Han, S. C., Doh, J. M., Yoon, J. K., Kim, G. H., Byun, J. Y., Han, S. H., Hong, K. T. and Kwun, S. I., Highly ordered self-organized TiO_2 nanotube arrays prepared by a multi-step anodic oxidation process**,** *Met. Mater. Int.,* 15, 493–499 (2009). https://doi.org/10.1007/s12540-009-0493-x

Jedi-soltanabadi, Z., Pishkar, N. and Ghoranneviss, M., Enhanced physical properties of the anodic TiO_2 nanotubes via proper anodization time, *J. Theorey Appl. Phy.*, 12(2), 135-139(2018). https://doi.org/10.1007/s40094-018-0290-3

Kahlmeter, G., An international survey of the antimicrobial susceptibility of pathogens from uncomplicated urinary tract infections: the ECO·SENS Project, *J. Antimicrob. Chemother*., 51, 69–76 (2003). https://doi.org/10.1093/jac/dkg028

Kunrath, M. F., Hübler, R., Shinkai, R. and Teixeira, E. R., TiO_2 nanotubes as an antibacterial nanotextured surface with potential for dental implants: Systematic review and meta-analysis, *Mater. Sci. Eng. C,* 40(6), 907-920(2024). https://doi.org/10.1016/j.dental.2024.04.009

Lai, C. W. and Sreekantan, S., Photoelectrochemical Performance of Smooth TiO_2 Nanotube Arrays: Effect of Anodization Temperature and Cleaning Methods, *Int. J. Photoenergy*, 2012(1), 356943 (2012). https://doi.org/10.1155/2012/356943

Mahmud, A. H., Habiballah, A. S. and Jani, A. M. M., The Effect of Applied Voltage and Anodisation Time on Anodized Aluminum Oxide Nanostructures, *Mater. Sci. Forum, Trans Tech Publ*., 819, 103–108 (2015). https://doi.org/10.4028/www.scientific.net/MSF.819.103

Mazzarolo, A., Lee, K., Vicenzo, A. and Schmuki, P., Anodic TiO_2 nanotubes: Influence of top morphology on their photocatalytic performance, *Electrochem. Commun.,* 22, 162–165 (2012). https://doi.org/10.1016/j.elecom.2012.05.037

Meyer, E., Jonas, D., Schwab, F., Rueden, H., Gastmeier, P. and Daschner, F. D., Design of a surveillance system of antibiotic use and bacterial resistance in German intensive care units (SARI), *Infect.,* 31(4), 208-215(2003). https://doi.org/10.1007/s15010-003-3201-7

Meyer, E., Schwab, F., Gastmeier, P., Rueden, H. and Daschner, F. D., Surveillance of antimicrobial use and antimicrobial resistance in German intensive care units (SARI): a summary of the data from 2001 through 2004, *Infect.,* 34(6), 303-309(2006). https://doi.org/10.1007/s15010-006-6619-x

Mohan, L., Dennis, C., Padmapriya, N., Anandan, C., and Rajendran, N. J. M. T. C., Effect of electrolyte temperature and anodization time on formation of TiO_2 nanotubes for biomedical applications, *Mater. Today Commun.,* 23, 101103(2020). https://doi.org/10.1016/j.mtcomm.2020.101103

Montakhab, E., Rashchi, F. and Sheibani, S., Modification and photocatalytic activity of open channel TiO_2 nanotubes array synthesized by anodization process, *Appl. Surf. Sci.,* 534, 147581 (2020). https://doi.org/10.1016/j.apsusc.2020.147581.

Opolot, E. E., Zhang, L., Abogodiri, S. O., Kumar, R., and Truong, V. T., Synergistic antibacterial activity and inhibition of TiO_2 nanotube array against multi-drug-resistant bacteria, *Front. Microbiol*., 15,616649(2024). https://doi.org/10.3389/fmicb.2024.618849

O'Toole, G. A., Microtiter dish biofilm formation assay, *J. Visual. Exp.,* (47), 2437(2011). https://doi.org/10.3791/2437

Pollán, M., Pérez-Gómez, B., Pastor-Barriuso, R., Oteo, J., Hernán, M. A., Pérez-Olmeda, P., Jose, L. S., Aurora, F. G., Isreal, C., Nerea, F. D. L., Marta, M., Francisco, R. C., Mariano, M. Paloma, M. A., Joose, L. P., Juan, F. M. M., Faustino, B. and Raquel, Y., 396(10250), 535–544 (2020). https://doi.org/10.1016/S0140-6736(20)31483-5

Rahimpour, N., Mollavali, M. and Rashidi, F., A Comprehensive Study on Synthesis Parameters of TiO_2 Nanotube Arrays: The Effects on Morphology and Photocatalytic Degradation of Para-NitroPhenol, *Phy. Chem, Res.,* 9(2), 261-279(2021). https://doi.org/10.22036/pcr.2021.257129.1853

Raja, D. H. and Arsha, A., Optical and morphological studies of Titania nanotubes and their characterizations, *Next Mater*., 4, 100215 (2024). https://doi.org/10.1016/j.nxmate.2024.100215

Rathi, A. K., Kmentová, H., Naldoni, A., Goswami, A., Gawande, M. B., Varma, R. S. and Zbořil, R., Significant enhancement of photoactivity in hybrid TiO_2/g-C_3N_4 nanorod catalysts modified with Cu–Ni-based nanostructures, *ACS Appl. Nano Mater.*, 1(6), 2526-2535(2018). https://doi.org/10.1021/acsanm.8b00078

Regonini, D., Satka, A., Jaroenworaluck, A., Allsopp, D. W. E., Bowen, C. R. and Stevens, R., Factors influencing surface morphology of anodized TiO_2 nanotubes, *Electrochim. Acta*, 74, 244–253 (2012). https://doi.org/10.1016/j.electacta.2012.04.076

Rojviroon, T., Rojviroon, O. and Sirivithayapakorn, S., Photocatalytic decolourisation of dyes using TiO_2 thin film photocatalysts, *Surf. Eng.*, 32(8), 562-569(2016). https://doi.org/10.1179/1743294415Y.0000000096

Sun, M., Fang, Y., Kong, Y., Sun, S., Yu, Z. and Umar, A., Graphitic carbon nitride (g-C_3N_4) coated titanium oxide nanotube arrays with enhanced photo-electrochemical performance, *Dalton Trans*., 45, 12702–12709 (2016). https://doi.org/10.1039/C6DT02071B

Surya, B., Ahmad, D. N. A., Sakti, H. H. and Sahban, H., Land Use Change, Spatial Interaction, and Sustainable Development in the Metropolitan Urban Areas, *Land*, 9(3), 95 (2020). https://doi.org/10.3390/land9030095

Torres, Á. I. P., Souza, R. M., Chino-Ulloa, A., Ruiz-Trabolsi, P. A., Tadeo-Rosas, R., Carrera-Espinoza, R. and Hernández, S. E., *Crystals*, 13(7), 1059 (2023). https://doi.org/10.3390/cryst13071059